# Adsorption of Weakly Charged Polyelectrolytes at Oppositely Charged Surfaces

**Per Linse**

*Physical Chemistry 1, Chemical Center, Lund University, P.O. Box 124, S-221 00 Lund, Sweden*

*Received April 17, 1995; Revised Manuscript Received September 22, 1995*[⊗]

ABSTRACT: The adsorption of weakly charged polyelectrolytes at planar and oppositely charged surfaces was modeled by using a mean-field lattice theory for flexible polyelectrolytes in solution. The nature of the adsorption was described in terms of volume fraction profiles, adsorbed amount, thickness of adsorbed layer, and conformational characteristics at different salt concentrations. The effect on the adsorption of (i) polyelectrolyte length, (ii) linear charge density of the polyelectrolyte, (iii) volume fraction of the polyelectrolyte, (iv) nonelectrostatic polyelectrolyte−surface interaction, and (v) surface potential or surface charge density, all at different salt concentrations and different surface conditions, was investigated. In most cases, as the salt concentration is increased, the adsorbed amount is reduced but the thickness of the adsorbed layer is increased. At low salt concentration and at constant surface charge density, the amount adsorbed is governed by the surface charge density through a polyelectrolyte−surface charge matching. At constant surface potential, a more diverse picture has emerged. A less regular distribution of the charges along the polyelectrolyte chain facilitates the adsorption.

## I. Introduction

Polyelectrolytes as well as polymers in general are used in a vast number of different applied areas and are likewise vital in biological systems. An overview of experimental and theoretical progress in the area of polymer (including polyelectrolytes) adsorption has recently been given by Fleer et al.[1] The adsorption of polyelectrolytes at large surfaces and on colloidal particles has been investigated by a range of experimental methods. It has since long been recognized that polyelectrolytes adsorb rather flat at an oppositely charged surface and that they are difficult to desorb even at high salt concentration. However, weakly charged (low linear charge density) polyelectrolytes display a thicker adsorbed layer and a richer behavior with respect to variation of molecular weight, addition of salt, and presence of nonelectrostatic interactions.[2−5]

On the theoretical side, the adsorption of polyelectrolytes at large surfaces and on colloidal particles has been a subject of great interest. Beside analytic theories of polyelectrolyte adsorption,[6−9] theoretical approaches as numerical solutions of mean-field lattice models[5,9−12] and Monte Carlo simulations[8,13−16] have been applied during recent years.

Recently, van de Steeg et al. made an extensive numerical investigation of the adsorption of polyelectrolytes at oppositely charged surfaces by using a mean-field lattice theory.[12] They introduced the concepts of "screening-enhanced adsorption" and "screening-reduced adsorption" regimes. These regimes apply to the cases where the adsorbed amount increases and decreases, respectively, upon an addition of salt. The former one is more typical for highly charged polyelectrolytes, i.e., in the case when adsorption is limited by electrostatic repulsion between the segments of the polyelectrolyte. Screening of this repulsion leads to an increase in polyion adsorptivity, provided the nonelectrostatic polymer−surface interaction is strong enough to keep the screened polyelectrolyte adsorbed. However, salt screens not only repulsion between charged segments of polyelectrolyte but also the electrostatic attraction between the segments and the surface. In the case when the adsorption is dominated by this electrostatic attraction (relatively high surface charge, low polyelectrolyte charge, and weak nonelectrostatic contribution), increase of electrolyte concentration results in a decreasing adsorption. Naturally, a full range of situations intermediate between the above two regimes is feasible, and this often leads to the adsorbed amount as a function of salt concentration displaying a maximum.[2,4]

In a recent contribution, the adsorption of weakly charged cationic polyacrylamide in aqueous solution on oxidized silica was investigated.[5] It was found that the measured adsorbed amount, being essentially constant at low electrolyte concentration, decreases at high salt content. Moreover, the onset of the decline in the adsorbed amount depended on the type of counterion. The ellipsometric thickness increased gradually with an increase of salt concentration and leveled off at high salt content. The experimental results were compared with model calculations within the framework of a mean-field lattice theory. A good description of the experimental observed adsorbed amount vs salt concentration and adsorbed thickness vs salt concentration was obtained by using a constant surface potential, a random distribution of the polyelectrolyte charges, and proper choices of realistic surface potential and Flory−Huggins $\chi$-parameters for the nonelectrostatic interactions.

The present work deals with the adsorption of weakly charged polyelectrolytes using the same theoretical approach but explores different conditions and spans a wider range of parameter values. The work also complements the related work by van de Steeg et al.[12] in various aspects. The main extensions or differences are as follows: (i) constant surface potential as well as constant surface charge density, (ii) much longer chain lengths (up to 10 000 segments), (iii) different arrangements of the charges on the polyelectrolyte, and (iv) analysis of the adsorbed thickness as well as of the loop, tail, and train characteristics.

Starting from a reference system, the effect of (i) the polyelectrolyte length, (ii) the linear charge density of the polyelectrolyte, (iii) the polyelectrolyte volume frac-

[⊗] Abstract published in *Advance ACS Abstracts,* November 15, 1995.

0024-9297/96/2229-0326$12.00/0 

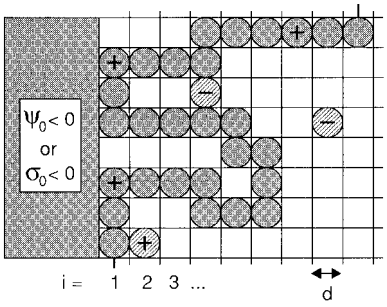


**Figure 1.** Illustration of a semi-infinite lattice bounded by a solid surface (shaded area) at which a part of a polyelectrolyte (shaded circles) is adsorbed, salt species (dashed circles), and the solvent (unfilled lattice cells). Moreover, *i* represents the number of the layer parallel to the surface and *d* the lattice spacing. The surface has either a constant surface potential or a constant surface charge density.

tion, (iv) the nonelectrostatic polyelectrolyte−surface interaction, and (v) the surface potential/charge density on the adsorbed amount and the thickness of adsorbed layer have been considered, all at different salt concentrations for different surface conditions. The model calculations show that the adsorbed amount can be rather different for the constant surface charge and constant surface potential conditions, respectively. In the former case, the amount adsorbed is governed by the polyelectrolyte−surface charge matching, except at very high salt concentrations, whereas for constant surface potential a more diverse picture is obtained. Moreover, for weakly charged polyelectrolytes the molecular length significantly affects the adsorption, which is not the case for highly charged polyelectrolytes.

The paper is organized as follows. The theoretical model of the present investigation is outlined briefly in the following section. In section III, the results are presented. The first part of section III deals with the state of the adsorbed and weakly charged polyelectrolyte as well as with the influence of the charge distribution on the adsorption. In the second part, results obtained from systematic changes of system parameters are presented. The main observations are extracted and discussed in section IV, and the paper ends with conclusions given in section V.

## II. Theoretical Model

The adsorption of polyelectrolytes at a planar and oppositely charged surface is modeled on the basis of a self-consistent-field theory, initially developed by Scheutjens and Fleer[17,18] and later extended to polyelectrolytes by Böhmer et al.[10] and by Israël.[9] We will here only give the main features of the theory; for more details the reader is referred to the original publications.

Briefly, the space adjacent to a planar surface is divided into layers, and each layer is further divided into lattice cells of equal size. Within each layer the Bragg−Williams approximation of random mixing is applied, and thus all sites in a layer are equivalent. One lattice cell contains either solvent, a solvated ion, or a polymer segment. The model contains five different species: neutral polymer segment, positively charged polymer segment, cation, anion, and solvent (see Figure 1).

The polyelectrolyte is considered to be a completely flexible chain consisting of $r_{\text{polymer}}$ segments and with $\tau r_{\text{polymer}}$ elementary charges. Three different distributions of the total polyelectrolyte charge will be considered: (i) smooth charge distribution, i.e., a fractional charge $|e|\tau$ on each segment; (ii) regular distribution, i.e., $\tau r_{\text{polymer}}$ charged segments evenly distributed and separated by blocks of neutral segments; and (iii) random distribution, i.e., the $\tau r_{\text{polymer}}$ charged segments randomly positioned along the chain. In addition, some results pertaining to the adsorption of a diblock copolymer consisting of one charged and one uncharged block will also be given. The polyelectrolyte with random charge distribution was represented by one chain with fixed charge sequence. Hence, the results will depend on the charge sequence selected, but the dependence was found to be very weak and of no importance in this work.

There are two different types of interactions in the model: electrostatic (charge−charge) and nonelectrostatic (the rest). The nonelectrostatic interaction between species in adjacent lattice sites is described by Flory−Huggins $\chi$-parameters.[19] The same description is used for the interaction between a species and the surface. The relation to the adsorption parameter $\chi_s$ is given, e.g., for the polymer by $\chi_s = -\lambda_{1,0}(\chi_{\text{polymer,surface}} - \chi_{\text{solvent,surface}})$, $\lambda_{1,0}$ being the fraction of all neighbors of a site in layer 1 which resides in the surface layer. Since a hexagonal lattice was selected, $\lambda_{1,0} = {}^1/_4$ was employed.

In line with the random-mixing approximation, the charged species (charged polyelectrolyte segments and salt species) are assumed to interact with an electrostatic potential of mean force, $\psi_i$, which depends only on the distance to the surface (layer number *i*). The potential of mean force is related to the charge density through Poisson's equation

$$\epsilon_0\epsilon_r\nabla^2\psi_i = \rho_i \tag{1}$$

where $\epsilon_0\epsilon_r$ is the dielectric permittivity of the medium, $\nabla^2$ the Laplacian, and $\rho_i$ the total charge density in layer *i*. The charges of the species are located to planes in the middle of each lattice layer, and the space between the charged planes is free of charge. A uniform dielectric permittivity is used.

The computation involves a self-consistent determination of the segment distribution (i.e., the distribution of each polymer segment, salt species, and water molecules outside the surface). The species volume fraction, $\phi_{Ai}$ (volume fraction of species *A* in layer *i*), is simply related to $n_{xsi}$, the number of sites in layer i occupied by segments of rank s (the *s*th segment in a chain) belonging to component *x* according to

$$\phi_{Ai} = \frac{1}{L}\sum_x\sum_{s=1}^{r_x}\delta_{A,t(x,s)}n_{xsi} \tag{2}$$

where *L* is the number of sites in a layer and $r_x$ is the number of segments in component *x* ($r_x = 1$ for salt species and water and $r_x = r_{\text{polymer}} > 1$ for the polyelectrolyte). The Kronecker $\delta$ selects only segments of rank *s* of component *x* if they are of type *A*.

The expression for the segment distribution is more complex, since the correct weight of all conformations, as well as the connectivity of the chains, has to be taken into account. Starting with the partition function, $n_{xsi}$ is obtained by using a matrix method and is given by[20]

$$n_{xsi} = C_x\{\mathbf{\Delta}_i^{\mathrm{T}}\cdot[\prod_{s'=r_x}^{s+1}(\mathbf{W}^{t(x,s')})^{\mathrm{T}}]\cdot\mathbf{s}\}\{\mathbf{\Delta}_i^{\mathrm{T}}\cdot[\prod_{s'=2}^{s}\mathbf{W}^{t(x,s')}]\cdot\mathbf{p}(x,1)\} \tag{3}$$

where $C_x$ is a normalization factor related to the bulk volume fraction of component *x*, $\mathbf{W}^{t(x,s)}$ is a tridiagonal matrix comprising elements which contain factors describing the lattice topology as well as weighting factors for each segment of rank *s* belonging to component *x*, and $\mathbf{p}(x,1)$ is a vector describing the distribution of the first segment of component *x* among the layers, $\mathbf{\Delta}$ and $\mathbf{s}$ being elementary column vectors. The weighting factor $G_{Ai}$ for species *A* in layer *i* entering $\mathbf{W}$ is given by

$$G_{Ai} = \exp(-\beta u_{Ai}) \tag{4}$$

where $\beta = 1/(kT)$ with *k* being the Boltzmann constant and *T* the absolute temperature. The species potential $u_{Ai}$ entering in eq 4 can be divided into two parts according to

$$u_{Ai} = u'_i + u_{Ai}^{\text{int}} \tag{5}$$

**Table 1. Parameters of the Reference System**[a]

| quantity | value |
|---|---|
| temperature | $T = 298$ K |
| relative dielectric constant | $\epsilon_r = 80$ |
| lattice spacing | $d = 6$ Å |
| regular distribution of polymer charges | |
| degree of polymerization | $r_{polymer} = 1000$ |
| fraction of charged segments | $\tau = 0.05$ |
| polymer volume fraction | $\phi_{polymer} = 1.0 \times 10^{-4}$ |
| salt volume fraction | $\phi_s = 1.0 \times 10^{-5}$ |
| surface potential | $\psi_0 = -50$ mV (if constant $\psi_0$) |
| surface charge density | $\sigma_0 = -0.03$ (if constant $\sigma_0$) |
| interaction parameters[b] | $RT\chi_{polymer,water} = 0.5RT$ |
| | $RT\chi_{polymer,cation} = 0.5RT$ |
| | $RT\chi_{polymer,anion} = 0.5RT$ |

[a] Conversion factors: Concentration (M) = $7.7\phi$ and surface charge (C m$^{-2}$) = $0.445\sigma_0$. [b] Other interaction parameters are zero.

and if the species potentials are defined with respect to the bulk solution with zero electrostatic potential, i.e., if $u_A^b = 0$, then the two terms are given by

$$\beta u'_i \equiv \alpha_i + \sum_x \frac{\phi_x^b}{r_x} + \frac{1}{2}\sum_{A'}\sum_{A''}\phi_{A'}^b \chi_{A'A''}\phi_{A''}^b$$

$$\beta u_{Ai}^{int} \equiv \sum_{A'}^{s} \chi_{AA'}(\langle\phi_{A'i}\rangle - \phi_{A'}^b) + \beta q_A \psi_i \qquad (6)$$

The angular brackets indicate an averaging over three adjacent layers and the superindex $s$ of the species summation symbol implies that the surface species is included in the sum as well. The species independent term $u'_i$ ensures that the space is completely filled in layer $i$ if a suitable choice of $\alpha_i$ is made, $u'_i$ being related in a continuous model to the lateral pressure. In bulk, $u'$ becomes zero. The species dependent term $u_{Ai}^{int}$ has two contributions: the mixing energy for species $A$ in layer $i$ being diminished by the mixing energy for species $A$ in bulk and the electrostatic energy of species $A$ carrying charge $q_A$ in the electrostatic potential $\psi_i$. At distances far from the surface, $\phi_{Ai}$ approaches $\phi_A^b$, $\psi_i$ approaches zero, and hence $u_{Ai}^{int}$ becomes zero. Since $u_{Ai}$ is needed for obtaining $\phi_{Ai}$ using eqs 2−4, and since $u_{Ai}$ depends in turn on $\phi_{Ai}$ according to eqs 5 and 6, eqs 2−6 need to be solved self-consistently. In addition, the electrostatic potential, which enters in eq 6 and depends on $\phi_{Ai}$, has to fulfill Poisson's equation (eq 1) with $\rho_i\sum_A q_A\phi_{Ai}$.

All calculations were performed for a model system at 298 K using a relative dielectric constant $\epsilon_r = 80$ and a lattice spacing $d = 6$ Å. Since a rather large set of parameters is needed to fully characterize a model system, the systems will be described by using one particular system as a reference system. If nothing else is stated, the polyelectrolyte contains 1000 segments and has 50 elementary charges ($\tau = 0.05$) regularly distributed. The polyelectrolyte volume fraction is $\phi_{polymer} = 1.0 \times 10^{-4}$ (on the adsorption plateau) and the volume fraction of the salt species (1:1 electrolyte) are $\phi_s = 1.0 \times 10^{-5}$ in addition to the volume fraction of the monovalent counterions of the polyelectrolyte. The polymer segments have unfavorable nonelectrostatic interactions ($\chi = 0.5$) with water and salt species, and the surface has no preferential interaction with any species. Moreover, the bare surface is modeled as having either (i) a fixed surface potential $\psi_0 = -50$ mV or (ii) a fixed surface charge density $\sigma_0 = -0.03$. For simplicity the former will often be referred to as the $\psi_0$-surface and the latter to as the $\sigma_0$-surface. For the reference system, the surface potential becomes −50 mV when the surface charge density is close to −0.03, but, of course, this relation does not generally hold for other conditions. The parameters for the reference system as well as conversion to real units are given in Table 1.

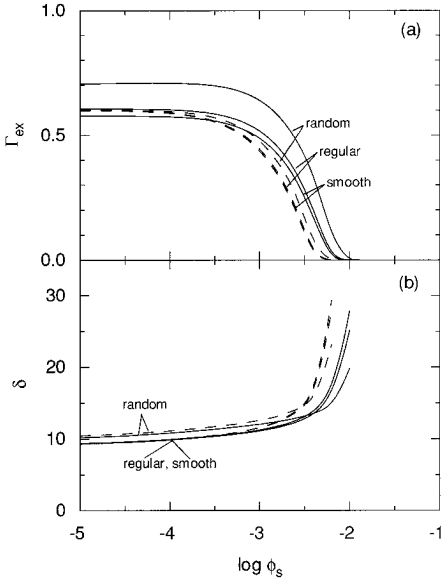


**Figure 2.** (a) Excess amount of adsorbed polyelectrolyte segments ($\Gamma_{ex}$) and (b) thickness of the adsorbed layer ($\delta$) versus the logarithm of the volume fraction of 1:1 salt ($\phi_s$) at constant surface potential $\psi_0 = -50$ mV (solid curves) or at constant surface charge density $\sigma_0 = -0.03$ (dashed curves) for smooth, regular, and random distributions of the charges along the polyelectrolyte chain. Other parameters are according to Table 1.

## III. Results and Analysis

In the first part, results describing the adsorbed state of the polyelectrolyte for the reference system are presented. Some data illustrating effects of the different charge distributions are also given. In the second part, it is examined how the adsorbed amount, thickness, and conformation changes with the length, the linear charge density, and the volume fraction of the polyelectrolyte as well as with the nonelectrostatic polyelectrolyte−surface interaction and the surface potential/charge density, all at different salt concentrations.

**Reference System. General Description and Effects of the Charge Distribution.** As indicated in the previous section, different distributions of the charged segments along the polyelectrolyte have been considered. Figure 2a shows the excess amount adsorbed, $\Gamma_{ex}$, in terms of equivalent number of monolayers as a function of the volume fraction of a 1:1 electrolyte using the reference system for (i) the smooth distribution of the total charge, (ii) the regular distribution of unit charges, and (iii) the random distribution of unit charges. The corresponding thickness, $\delta$, defined as twice the first moment of the excess polymer volume fraction profile as a function of the salt volume fraction is given in Figure 2b. Moreover, Table 2 gives the excess amount adsorbed, the degree of surface charge compensation expressed by the ratio of the charge of the adsorbed polyelectrolyte and the surface charge, $\tau\Gamma_{ex}/|\sigma_0|$, and the thickness of the adsorbed layer, all at low salt concentration, as well as $\phi_{s,1/2}$, the salt volume fraction at which $\Gamma_{ex}$ is reduced to half its maximal value. Data for the diblock copolymer with one charged and one uncharged block are also included in Table 2.

For this case of pure electrosorption, and with disregard for the different charge distributions and types of surfaces for the moment, Figure 2a shows that the adsorbed amount is constant at low salt concentration and reduces to zero at increasing salt concentration. This behavior has been coined as the screening-reduced

**Table 2. Excess Adsorbed Amount, $\Gamma_{ex}$, Degree of Surface Charge Compensation, $\tau\Gamma_{ex}/|\sigma_0|$, and Thickness of Excess Adsorbed Layer, $\delta$, at $\phi_s = 10^{-5}$ as Well as Salt Volume Fraction at Which $\Gamma_{ex}$ Has Reduced to Half Its Maximal Value, $\phi_{s,1/2}$, for Surface with Constant Potential or with Constant Charge Density[a]**

| charge distribution | $\psi_0 = -50$ mV | | | | $\sigma_0 = -0.03$ | | | |
|---|---|---|---|---|---|---|---|---|
| | $\Gamma_{ex}$ | $\Gamma_{ex}/\lvert\sigma_0\rvert$ | $\delta$ | $10^3\phi_{s,1/2}$ | $\Gamma_{ex}$ | $\tau\Gamma_{ex}/\lvert\sigma_0\rvert$ | $\delta$ | $10^3\phi_{s,1/2}$ |
| smooth | 0.5774 | 0.9990 | 9.39 | 2.75 | 0.5995 | 0.9992 | 9.30 | 1.84 |
| regular | 0.6049 | 0.9995 | 9.33 | 2.97 | 0.5996 | 0.9993 | 9.35 | 1.92 |
| random | 0.7062 | 1.0014 | 10.2 | 3.73 | 0.6005 | 1.0008 | 10.5 | 2.24 |
| diblock | 1.813 | 0.9999 | 41.6 | 33.0 | 0.5991 | 0.9985 | 39.0 | 8.68 |

[a] $\Gamma_{ex} \equiv \Sigma_i (\phi_i - \phi^b)$ and $\delta \equiv 2\Sigma_i i(\phi_i - \phi^b)/\Sigma_i (\phi_i - \phi^b)$, where $\phi_i$ and $\phi^b$ are the polyelectrolyte volume fractions in layer $i$ and in bulk, respectively.

adsorption regime.[12] The adsorption is driven by the attractive electrostatic interaction between the polyelectrolyte and the surface, and upon an increase of the salt concentration, this attraction is screened. At some salt concentration, the electrostatic polyelectrolyte−surface attraction is balanced by the entropic cost of the polyelectrolyte being close to the surface and the repulsive electrostatic interaction among the polyelectrolyte charges. The latter is of course also screened by the increased salt content. Figure 2b displays that the thickness has the opposite salt dependence. Thus, at increased salt concentration the *reduction of the excess amount adsorbed* is accompanied by an *increase in the thickness* of the adsorbed layer.

Furthermore, Figure 2a and Table 2 show that, for the $\psi_0$-surface, $\Gamma_{ex}$ as well as $\phi_{s,1/2}$ increases as the charge distribution of the polyelectrolyte becomes more uneven. Whereas the difference between the smooth and the regular distribution is small, the increase in the adsorbed amount for the random distribution is significant, ca. 15%. The salt concentration at which the adsorbed amount has reduced to half its maximal value, $\phi_{s,1/2}$, is increased by 25%. For an even more uneven charge distribution, the increase in the adsorbed amount and the resistance to added salt become dramatic. In the limit of the diblock copolymer, $\Gamma_{ex}$ increases 3-fold and $\phi_{s,1/2}$ 11-fold. Regarding the thickness of the adsorbed layer, the trends are similar. Figure 2b shows that, at low $\phi_s$, the thickness for the random distribution is ca. 10% larger than that for the smooth and regular distributions, whereas, at such high $\phi_s$ that $\Gamma_{ex} < 0.1$, the thickness of the adsorbed layer for the random distribution approaches that of the other two for same $\Gamma_{ex}$. For the $\sigma_0$-surface, Figure 2 and Table 2 show that at low salt concentration (i) the adsorbed amount is essentially independent of the charge distribution (even considering the diblock copolymer), (ii) the thicknesses are very close to those for the $\psi_0$-surface, and (iii) the increase of $\phi_{s,1/2}$ in the sequence: smooth, regular, and random charge distribution is smaller as compared to the $\psi_0$-surface.

The theory makes it possible to make a detailed analysis of the occurrence of loops, tails, and trains of the adsorbed polyelectrolyte.[18] Figure 3a shows the average length of loops and tails (average number of segments in one loop and in one tail) as a function of the salt concentration for the reference system with the $\psi_0$-surface, whereas Figure 3b displays the average fraction of segments being in loops, tails, or trains. Again,with initial disregard for the difference among the various charge distributions, Figure 3a shows that at low $\phi_s$ the average tail size is ca. 100 segments (10% of the chain length) and increases to ca. 300 when $\Gamma_{ex}$ approaches zero. The average loop length is considerably shorter, ca. 28 segments, and increases to ca. 40 at $\Gamma_{ex} \approx 0$. The average train length remains between 2 and 3 at all $\phi_s$ (not shown). As seen from Figure 3b,

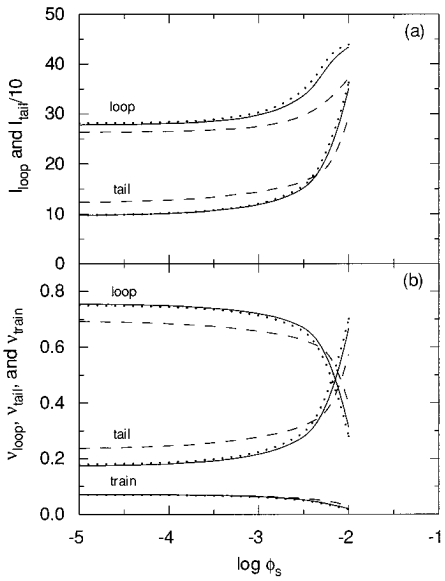


**Figure 3.** (a) Average length of loops and tails (l) and (b) fraction of polyelectrolyte segments being in loops, tails, and trains ($\nu$) versus the logarithm of the volume fraction of 1:1 salt ($\phi_s$) at constant surface potential $\psi_0 = -50$ mV for smooth (dotted curves), regular (solid curves), and random (dashed curves) distributions of the charges along the polyelectrolyte chain. Other parameters are according to Table 1.

at low $\phi_s$ the large majority of the segments are to be found in loops (ca. 75%), about 8% in trains and the rest in tails. At increased salt concentration, the fractions in loops and trains are reduced and the fraction in tails is increased. At $\Gamma_{ex} \approx 0$, only 30% of the segments remains in loops, 2.5% is in contact with the surface, and ca. 60−65% is in tails. The average number of loops is 28 at low $\phi_s$ and reduces to ca. 11 at $\Gamma_{ex} \approx 0$.

Figure 3 also gives the corresponding quantities for polyelectrolytes with different charge distributions. Again the differences between the smooth and the regular arrangements are small, and the results for the random distribution deviate from those of the other two distributions. The fraction of segments being in loops is smaller and the fraction being in tails is larger, resulting in a reduction of the average loop length and an increase of the average tail length. The direction of these changes might again be understood when the limit of the diblock copolymer is considered. In this limit, the average loop and tail lengths become 12 and 600, respectively, and the average fractions of segments in loops and tails are 0.09 and 0.87, respectively, all quantities being independent of the salt concentration up to $\phi_s = 0.08$ (corresponding to $\Gamma_{ex} \approx 0$).

**Reference System. Potential Profiles.** The reduced electrostatic potential as a function of the distance from the charged surface for the reference system at constant surface potential $\psi_0 = -50$ mV, corresponding to $e\psi_0/kT = 1.95$, is shown in Figure 4. The potential

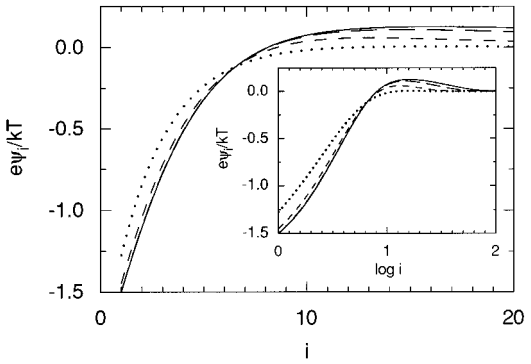


**Figure 4.** Reduced electrostatic potential ($e\psi_i/kT$) versus the layer number ($i$) for $\phi_s = 10^{-5}$ (solid curve), $10^{-4}$ (long dashed curve), $10^{-3}$ (short dashed curve), and $5 \times 10^{-3}$ (dotted curve) at constant surface potential $\psi_0 = -50$ mV. The inset shows the same data on a log−lin scale. Other parameters are according to Table 1.

is negative close to the surface but changes sign further out ($i \approx 8$) and approaches zero from above at large distances.

In the inner region ($i < 8$) and for $\phi_s < 10^{-3}$, the amplitude of the potential decays somewhat faster than exponentially, and the potential profile is essentially independent of the salt concentration. At the highest salt concentration considered here, $\phi_s = 5 \times 10^{-3}$, the potential becomes exponentially decaying. This salt concentration corresponds to the case where the adsorbed amount has reduced by a factor of 4 from its maximum value (cf. Figure 2a).

On the other hand, in the outer region ($i > 16$) the decay from the maximum to zero with increasing distance is fairly exponential and depends on the electrolyte concentration, even at low $\phi_s$. The obtained decay lengths are $\kappa^{-1} = 17$, 12, and 6 layers for $\phi_s = 10^{-5}$, $10^{-4}$, and $10^{-3}$, respectively. Using $d = 6$ Å and the conversion factor $c_s/M = 7.7\phi_s$, the Debye screening lengths originating from the salt become $\kappa_s^{-1} = 56$, 18, and 6 layers, respectively. At low $\phi_s$, $\kappa^{-1} \ll \kappa_s^{-1}$ is obtained, and hence the decay length is determined by the polyelectrolyte, whereas at high $\phi_s$ we get $\kappa^{-1} \approx \kappa_s^{-1}$ and the contribution from the salt dominates. At $\phi_s = 10^{-4}$, $\kappa^{-2} \approx 2\kappa_s^{-2}$, and thus the polyelectrolyte and the added salt contribute roughly equally to the screening length. This salt volume fraction is 20 times larger than the volume fraction of polyelectrolyte charges and its counterions.

The nonmonotonic behavior of the potential is typically found for electrostatically strongly coupled systems. The observed maximum of the electrostatic potential at a given layer ($i \approx 16$) signals a charge inversion, i.e., the absolute value of the net charge of the components in the region extending from the fist layer to the given one exceeds that of the charged surface. For $\phi_s = 10^{-5}$, the maximal charge reversal is 0.8% of the surface charge and occurs in layer 26. The magnitude of the charge reversal reduces with added salt; at $\phi_s = 5 \times 10^{-3}$ it is 1 order of magnitude smaller. However, there is no significant overcompensation of the surface charges by the oppositely charged polyelectrolyte *alone*; it is the charge from the polyelectrolyte and the similarly charged ions together which exceeds the amplitude of the surface charge (cf. Table 2).

Thus, at not too high salt concentration a small charge inversion is obtained when considering all charged species. At the lowest salt concentration considered, the 1:1 electrolyte only marginally contributes to the screening of the surface potential, but at intermediate concentrations, the electrolyte dominates the screening in the outer region. At even higher salt concentrations, the magnitude of the charge inversion decreases rapidly and the electrolyte starts to contribute to the electrostatic screening even close to the surface. At this stage the amount of adsorbed polyelectrolyte has substantially decreased from its maximal value.

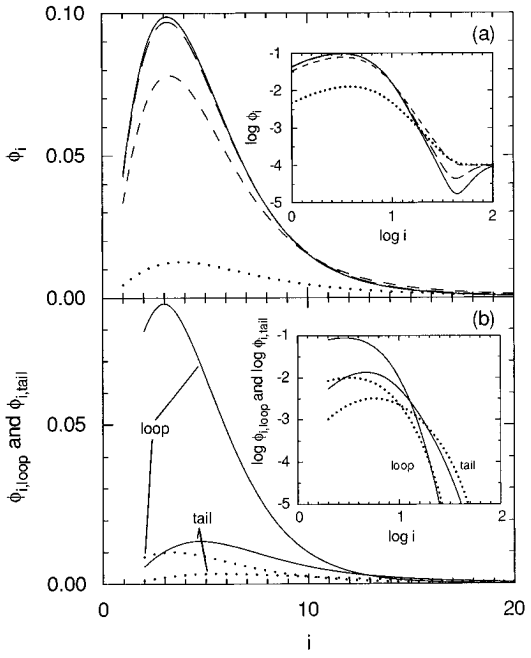


**Figure 5.** (a) Volume fraction of polymer segments ($\phi_i$) and (b) volume fraction of polymer segments in loops and tails ($\phi_{iloop}$ and $\phi_{itail}$) versus the layer number ($i$) for $\phi_s = 10^{-5}$ (solid curve), $10^{-4}$ (long dashed curve), $10^{-3}$ (short dashed curve), and $5 \times 10^{-3}$ (dotted curve) at constant surface potential $\psi_0 = -50$ mV. In b data for only two salt concentrations are given. The insets show the same data on a log−log scale. Other parameters are according to Table 1.

The occurrence of charge reversal has been indirectly demonstrated by direct measurements of the force between mica surfaces separated by aqueous solution of highly charged cationic polyelectrolyte.[21] However, in this system nonelectrostatic surface−polyelectrolyte interactions are operating as well.

**Reference System. Concentration Profiles.** The corresponding total polymer volume fraction profiles as well as the profiles of segments being in loops and tails are shown in Figure 5. At this rather weak adsorption of the weakly charged polyelectrolyte, Figure 5a shows that the maximum of the total volume fraction occurs a few layers into the solution. Even at the lowest $\phi_s$, where the maximal $\Gamma_{ex}$ is obtained, the volume fraction does not exceed 0.1, thus the adsorbed layer is dilute. The corresponding data are given in a log−log representation in the inset. At intermediate distance ($i \approx 10-40$), the total polymer volume fraction decays according to the power law $\phi_{polymer} \approx i^x$ with $x$ being salt dependent, decreasing from $x = -5.3$ at $\phi_s = 10^{-5}$ to $x = -2.8$ at $\phi_s = 5 \times 10^{-3}$. The depletion zone, appearing at the outer part of the adsorbed layer at low $\phi_s$, vanishes gradually at increasing $\phi_s$.

From Figure 5b it is clear that the main part of the adsorbed layer is formed by the segments being in loops, as already could be inferred from the large fraction of loops segments (cf. Figure 3b). At the onset of the intermediate region where the power law starts ($i \approx 10$), the contribution from segments in loops and tails

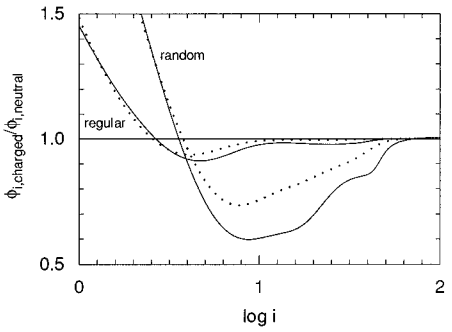


**Figure 6.** Ratio of volume fraction of charged polymer segments to neutral polymer segments ($\phi_{icharge}/\phi_{ineutral}$), normalized to one in bulk, versus the logarithm of the layer number ($i$) at constant surface potential $\psi_0 = -50$ mV for $\phi_s = 10^{-5}$ (solid curves) and $5 \times 10^{-3}$ (dotted curves) for regular and random charge distributions of the charges along the polyelectrolyte chain. Other parameters are according to Table 1.

becomes comparable. At this distance the volume fraction of loop segments has reduced to about a tenth of its maximal value, and at larger distances the contribution from the segments in loops to the total volume fraction profile decreases rapidly. Despite the fact that tail segments are more numerous than loop segments at $i > 10$, the vast majority of the tail segments is to be found close to the surface ($i < 10$). The spatial extension of the loop layer is similar at the two salt concentrations, but the extension of the tail segments is larger at the higher $\phi_s$. This causes the crossover of the loop and tail volume fractions to occur at shorter distance and the tail of the total volume fraction profile to protrude more from the surface. This is consistent with the following: (i) that at low salt concentration ($\phi_s = 10^{-5}$) the extension of the loop layer agrees with twice the first moment of the volume fraction profile ($\delta = 9.3$) and (ii) that at high salt concentration ($\phi_s = 5 \times 10^{-3}$) the contribution from the tail segments is responsible for the increased thickness from $\delta = 9.3$ to $\delta = 16$.

In contrast to the polyelectrolyte segments, the volume fraction profiles of the salt species follow closely the Boltzmann weight of the electrostatic potential (not shown), since (i) the salt species are not connected and (ii) the nonelectrostatic contribution is of minor importance due to the fact that the system is dilute and that the surface interaction parameters are zero.

The unequal interaction with the electrostatic field tends to create a spatial segregation of the charged and neutral segments with respect to the distance to the surface. Figure 6 shows on a log−lin scale the ratio of the volume fractions of charged and neutral polyelectrolyte segments (normalized to one in bulk) for the regular and the random charge distributions. It is obvious that (i) a considerable segment segregation occurs, (ii) the segregation depends on the charge distribution, and (iii) it also depends on the salt concentration. Close to the surface charged segments are preferentially accumulated due to the electrostatic attraction between them and the oppositely charged surface, whereas further out there is an excess of neutral segments.

For the regular charge distribution, there is a surplus of charged segments only in the first two layers, and the largest deficiency in charged segments occurs at $i \approx 4-5$. At the lower salt concentration, $\phi_s = 10^{-5}$, the rise of the ratio to one from below display a weak maximum at $i \approx 10-15$. This maximum is likely due to fairly stretched neutral blocks with one adjacent charge at the surface and the other one at $i \approx 10-15$. Moreover, the maximum appears at the same location where the potential has a maximum. Thus, it is tentative to conclude that these two features are related. As $\phi_s$ is increased, the segregation is reduced by electrostatic screening. At $\phi_s = 5 \times 10^{-3}$ both the maxima in $\phi_{icharged}/\phi_{ineutral}$ and $e\psi_i/kT$ at $i \approx 10-15$ have disappeared. On the other hand, for the random charge distribution the segment segregation is much stronger. The $\phi_{icharged}/\phi_{ineutral}$ ratio reaches 2.4 in the first layer, independently of the salt concentration, and the minimum appears further away from the surface ($i \approx 9$) and is much deeper. At the lower $\phi_s$, the ratio profile displays several inflection points, and as for the regular distribution the depth is reduced at increasing salt concentration.

Thus, the model suggests that the adsorbed polyelectrolyte layer contains three regions, one close to the surface where the volume fraction display a maximum slightly outside the surface, one intermediate region where the volume fraction profile decays rapidly according to a power law, and one outer region where the volume fraction approaches its bulk value. In the inner region the loop segments dominate, whereas, in the intermediate region, the tail segments are more abundant. The exponent of the power law in the intermediate region is more negative than that predicted from scaling theory for adsorbed homopolymers in Θ-solvent ($-1$) and in good solvent ($-4/3$) or from mean-field theory in good solvent ($-2$) in the semidilute regime.[1] The presence of charged and uncharged polyelectrolyte segments makes it possible to obtain segment segregation. The spatial segregation can be rather intricate and increases as the linear charge distribution becomes more uneven and at lower salt concentration. For the case with a regular alternation of charged segments and blocks of 19 neutral segments, it is not possible to create large regions with a widely different ratio of charged to neutral polymer segments.

**Variation of the Length of the Polyelectrolyte.** We will now examine how the adsorption is influenced by the length of the polyelectrolyte. In the reference system the polyelectrolyte has 1000 segments, i.e., a molecular mass of the order $10^4-10^5$. Figure 7 shows the adsorbed amount for $r_{polymer} = 10\,000$ as a function of the salt concentration at fixed surface potential or charge density with otherwise identical conditions. The adsorbed amount and thickness as a function of the number of segments in the range of 100 to 10 000 at three salt concentrations are shown in Figure 8.

For $r_{polymer} = 10\,000$, Figure 7 shows that at low $\phi_s$ the amount adsorbed increases by 10% at constant surface potential and remains at $\Gamma_{ex} = 0.60$ at constant surface charge density. In addition, the amount of salt needed to displace the polyelectrolyte increases by ca. 100 and 50%, respectively. In the case of constant surface charge density at low $\phi_s$, Figure 8a clearly shows that the adsorbed amount is almost unaffected of the polymer length in the interval studied. At increased salt concentration the polyelectrolyte starts to desorb, the shorter chains doing so first. On the other hand, the adsorbed amount at the $\psi_0$-surface is more sensitive to the polyelectrolyte length ($\Gamma_{ex}$ increases with $r_{polymer}$) as compared to the $\sigma_0$-surface. For short polyelectrolytes the amount adsorbed is small even at low $\phi_s$.

The corresponding thickness of the adsorbed layer as a function of the polymer length is shown in Figure 8b

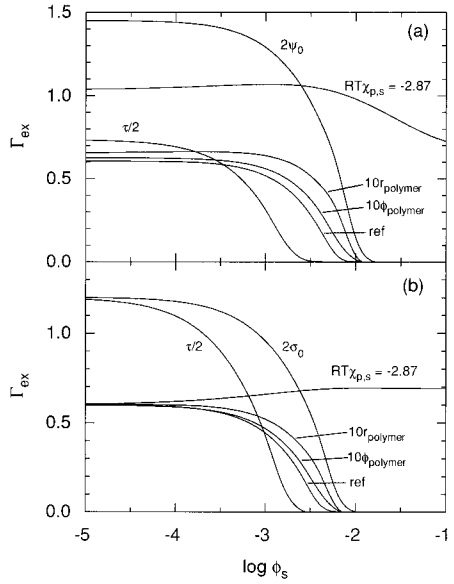


**Figure 7.** Excess amount of adsorbed polyelectrolyte segments ($\Gamma_{ex}$) versus the logarithm of the volume fraction of 1:1 salt ($\phi_s$) at (a) constant surface potential $\psi_0 = -50$ mV and (b) constant surface charge density $\sigma_0 = -0.03$ for the reference system (curve labeled ref) and for cases where one parameter is changed. The change of the parameters with respect to the reference system is indicated. Other parameters are according to Table 1.

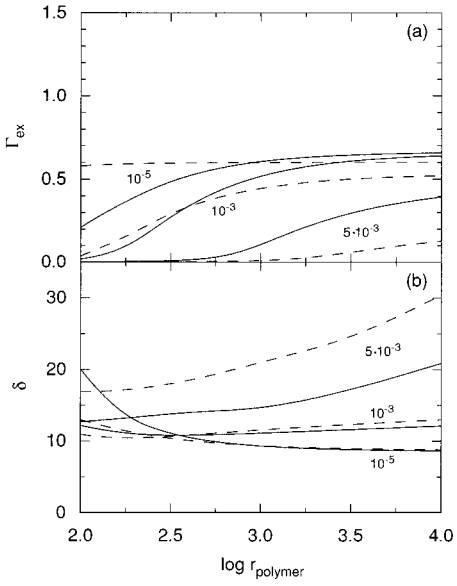


**Figure 8.** (a) Excess amount of adsorbed polyelectrolyte segments ($\Gamma_{ex}$) and (b) thickness of adsorbed layer ($\delta$) versus the logarithm of the number of segments of the polyelectrolyte ($r$(polymer)) at indicated salt volume fractions at constant surface potential $\psi_0 = -50$ mV (solid curves) and at constant surface charge density $\sigma_0 = -0.03$ (dashed curves). Other parameters are according to Table 1.

and displays some interesting features. Starting with low $r_{polymer}$, we observe a reduction of the thickness of the excess amount as the length increases for $\phi_s \leq 10^{-3}$. The contraction is most pronounced at low $\phi_s$ and for constant surface potential. For longer polyelectrolytes at high salt concentration ($\phi_s \geq 10^{-3}$), the thickness increases with $r_{polymer}$, in particular at the highest salt concentration where the adsorbed amount is small. Thus, the increase in thickness at addition of salt, as was shown in Figure 2b, becomes more accentuated for longer polyelectrolytes but is small or vanishes for shorter ones.

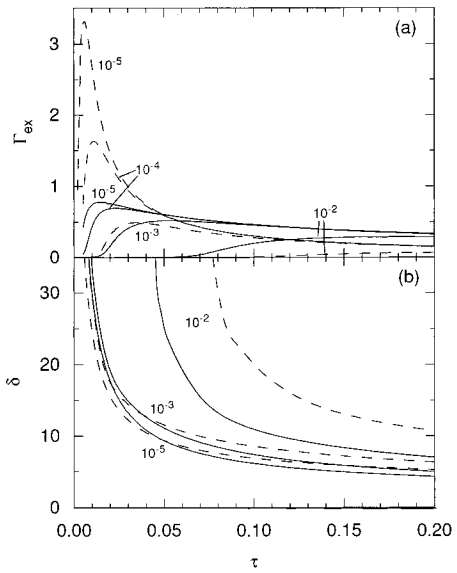


**Figure 9.** (a) Excess amount of adsorbed polyelectrolyte segments ($\Gamma_{ex}$) and (b) thickness of adsorbed layer ($\delta$) versus the fraction of charged segments of the polyelectrolyte ($\tau$) at indicated salt volume fractions at constant surface potential $\psi_0 = -50$ mV (solid curves) and at constant surface charge density $\sigma_0 = -0.03$ (dashed curves). Other parameters are according to Table 1.

The larger enhancement of the thickness for longer polyelectrolytes at increasing salt concentration is caused by a larger increase in the average loop and tail lengths for the longer chains. At $\phi_s = 10^{-5}$ the average loop and tail lengths differ only by ca. 10% between $r_{polymer} = 1000$ and $r_{polymer} = 10\,000$, and Figure 8b shows essentially the same thickness for these two chain lengths. However, at $\phi_s = 5 \times 10^{-3}$, the ratios of the average loop and tail lengths for $r_{polymer} = 10\,000$ and 1000 become 1.6 and 3.4, respectively, ($\psi_0$-surface) and 2.3 and 3.9, respectively ($\sigma_0$-surface); thus a considerable extension of, in particular, the average tail lengths is obtained. Similar changes at increased salt concentration of the differences of the adsorbed states between $r_{polymer} = 1000$ and $r_{polymer} = 10\,000$ was observed for a related system with an attractive nonelectrostatic polyelectrolyte−surface interaction at a $\psi_0$-surface. The results were interpreted that the longer polyelectrolyte could form more extended tails which strongly contributed to the increase in thickness but still having sufficient anchoring.[5]

**Variation of the Linear Charge Density of the Polyelectrolyte.** As for the variation of $r_{polymer}$, the adsorbed amount as a function of the salt concentration for a change in the linear charge density (reduction by a factor of 2) is shown in Figure 7, whereas $\Gamma_{ex}$ and $\delta$ as functions of $\tau$ for some $\phi_s$-values are given in Figure 9.

For the $\sigma_0$-surface, Figures 7b and 9 show that the adsorbed amount is proportional to the inverse linear charge density for sufficiently low $\phi_s$; thus, again $\Gamma_{ex}$ is governed by charge compensation. This holds even for $\tau$ as low as 0.005 (five charges on the polyelectrolyte), where $\phi_s = 10^{-5}$ is required. As the electrolyte concentration is increased, the polyelectrolytes with small $\tau$ cease to adsorb. At $\phi_s = 10^{-3}$, the maximal adsorption occurs at $\tau \approx 0.03$, and the adsorbed amount is strongly reduced, as compared to smaller $\tau$ at lower $\phi_s$, due to the fact that fewer neutral segments accompany each anchoring charged segment. The picture becomes drastically different for the case of the constant surface potential. The main differences are that (i) $\Gamma_{ex}$ depends

much less on $\tau$ and (ii) at low $\tau$ $\Gamma_{ex}$ is much less sensitive on $\phi_s$, as compared to the $\sigma_0$-surface. For example, at $\phi_s = 10^{-5}$, the maximum $\Gamma_{ex}$, which occurs at $\tau = 0.015$, is only twice that at $\tau = 0.2$, whereas for the $\sigma_0$-surface the corresponding ratio is ca. 15.

Despite the condition that $\Gamma_{ex}$ depends strongly on the salt concentration in the range $10^{-5}-10^{-3}$ and on the type of the surface, the thickness of the adsorbed layer varies essentially as $1/\tau$ and depends remarkably very little on the salt concentration or on the type of surface (see Figure 9b). These inverse $\tau$-dependencies displayed by the thickness originate of course from the fact that there are $1/\tau - 1$ neutral (and nonadsorbing) segments between each pair of adsorbing charged segments.

The large variation of the thickness is again reflected in the conformation characteristics. At $\phi_s = 10^{-5}$ with $\tau = 0.01$, ca. 30, 70, and 1% of the segments are in loops, tails, and trains, respectively, and the average loop and tail lengths are 55 and 350 segments, respectively. At $\tau = 0.2$, the fraction of segments in the different groups have changed to 70, 3, and 25%, respectively, with ca. 9 and 25 segments in the average loop and tail, respectively. Thus, the large thickness occurring at low $\tau$ is due to that more than $^2/_3$ of the whole polyelectrolyte form two long and extended tails and the rest few short loops. On the other hand, at $\tau = 0.2$, the tails have become negligible and the thickness is governed by the extension of the loop layer. At even larger $\tau$, we approach the limit of highly charged polyelectrolyte where the adsorbed layer is very thin and the adsorbed amount small. The difference in conformation characteristics between the $\psi_0$- and $\sigma_0$-surfaces is not prominent, as expected from Figure 9b, and the data given above are averaged over the two types of surfaces.

**Variation of the Polyelectrolyte Volume Fraction.** As previously demonstrated,[6] the adsorption isotherms of polyelectrolytes at charged surfaces are of a high-affinity type, and the plateau value is reached at extremely low polyelectrolyte concentration. Figure 7 shows that an increase of $\phi_{polymer}$ from $10^{-4}$ to $10^{-3}$ increases $\Gamma_{ex}$ slightly ($\psi_0$-surface) or leaves $\Gamma_{ex}$ unaffected ($\sigma_0$-surface) at low $\phi_s$ and increases $\phi_{s,1/2}$ by ca. 20−30%. Conformational analysis for $\phi_s = 10^{-5}$ shows that below $\phi_{polymer} = 10^{-3}$ there are no changes, whereas above variations start to occur. A 10-fold increase of $\phi_{polymer}$ from $10^{-3}$ to $10^{-2}$ causes the tail length to increase from 100 to 180 segments, whereas the average loop length remains constant, but the number of loops is reduced by 20%. The fraction of segments in trains or the length of the trains are not changed. The thickness of the adsorbed layer remains 9−10 layers at $\phi_s = 10^{-5}$ and 10−12 layers at $\phi_s = 10^{-3}$ for the interval $\phi_{polymer} = 10^{-5}-10^{-2}$. The conformational data are applicable to both types of surfaces, despite the fact that the adsorbed amount is larger and the thickness of the adsorbed layer slightly smaller for the $\psi_0$-surface at high $\phi_s$.

**Variation of the Nonelectrostatic Polyelectrolyte−Surface Interaction.** So far, we have only considered nonpreferential interacting surfaces. In the case where the polyelectrolyte has a favorable nonelectrostatic interaction with the surface, the adsorbed amount is expected to increase. In the absence of electrostatic interactions, there exists a critical surface interaction parameter, $\chi_s = \chi_{sc} = -\ln(1 - \lambda_{1,0}) \approx 0.288$, at which the adsorbed amount increases drastically for an infinitely long polymer.[1]

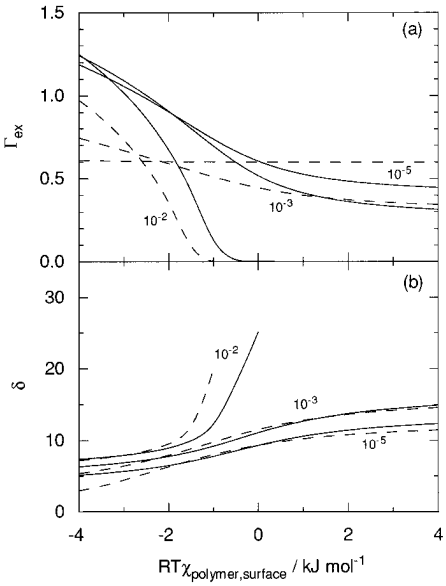


**Figure 10.** (a) Excess amount of adsorbed polyelectrolyte segments ($\Gamma_{ex}$) and (b) thickness of adsorbed layer ($\delta$) versus the polyelectrolyte−surface nonelectrostatic interaction parameter ($RT\chi$(polymer,surface)) at indicated salt volume fractions at constant surface potential $\psi_0 = -50$ mV (solid curves) and at constant surface charge density $\sigma_0 = -0.03$ (dashed curves). Other parameters are according to Table 1.

For our system with electrostatic interactions, Figure 7a shows that, at constant surface potential conditions, (i) the adsorbed amount is almost doubled when $RT\chi_{polymer,surface}$ is lowered from 0 to $-2.87$ kJ mol$^{-1}$ ($\chi_s \approx \chi_{sc}$) and (ii) independent of $\phi_s$ except at very high $\phi_s$ where $\Gamma_{ex}$ starts to decrease. For the surface with constant surface charge density, the same change in $\chi_{polymer,surface}$ (i) does not affect $\Gamma_{ex}$ at low $\phi_s$ and (ii) makes $\Gamma_{ex}$ to increase slightly with increasing $\phi_s$. Thus, we are roughly on the boarder between the screening-reduced adsorption and the screening-enhanced adsorption regime.[12]

Figure 10a shows that for the $\psi_0$-surface, $\Gamma_{ex}$ is strongly dependent on $RT\chi_{polymer,surface}$ for an attractive interaction and that $\Gamma_{ex}$ is reduced at repulsive polyelectrolyte-surface interaction. Of course, as $\phi_s$ is increased, desorption starts to take place, initially at positive $\chi_{polymer,surface}$, but as $\phi_s$ is increased even more, the adsorption−desorption transition becomes sharper and closer to $\chi_{sc}$. On the other hand, for the $\sigma_0$-surface, $\Gamma_{ex}$ is independent of $\chi_{polymer,surface}$ for $\phi_s < 10^{-4}$ and starts to depend on $RT\chi_{polymer,surface}$ first at higher salt concentrations. At these higher concentrations, the salt is able to electrostatically accommodate an overcompensated surface ($\Gamma_{ex} > 0.6$).

Figure 10b displays that the corresponding thicknesses of the adsorbed layers are smallest at large negative $RT\chi_{polymer,surface}$-values and increases with $RT\chi_{polymer,surface}$. As for the $\tau$-dependency, there are no pronounced differences between the types of surfaces or at different salt concentrations despite the differences in $\Gamma_{ex}$ (as long there are adsorbed polyelectrolytes left).

At $\phi_s = 10^{-5}$, the fraction of segments in loops, tails, and trains changes from 60, 5, and 35% to 55, 50, and 2%, respectively, as $RT\chi_{polymer,surface}$ increases from $-4$ to $+4$ kJ mol$^{-1}$. The fraction in loops displays a maximum of 75% at $\chi_{polymer,surface} \approx 0$. For the same variation in $RT\chi_{polymer,surface}$, the average lengths of loops and tails increase from 7 and 30, respectively, to 100 and 250, respectively. Thus, as $RT\chi_{polymer,surface}$ in-

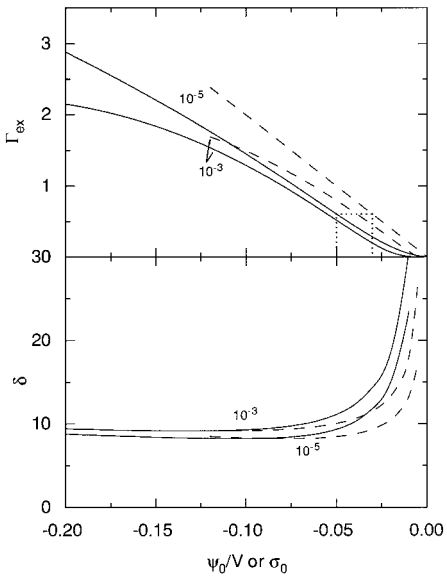


**Figure 11.** (a) Excess amount of adsorbed polyelectrolyte segments ($\Gamma_{ex}$) and (b) thickness of adsorbed layer ($\delta$) versus the surface potential ($\psi_0$) at constant surface potential (solid curves) and versus the surface charge density ($\sigma_0$) at constant surface charge density (dashed curves) at indicated salt concentrations. Other parameters are according to Table 1. The construction of the corresponding $\psi_0$- and $\sigma_0$-values for $\psi_0 = -50$ mV corresponding to $\sigma_0 \approx -0.03$ at $\phi_s = 10^{-5}$ is also shown (dotted lines).

creases from $-4$ to $+4$ kJ mol$^{-1}$, there is a dramatic change *from* a flat adsorbed state with every third segment of the adsorbed polyelectrolyte in the first layer and with ca. 90 short loops and 2 short tails *to* an extended state with much fewer anchoring points and with ca. 6 long loops and 2 long tails. Again, the data are averaged over the two surface types. At $\chi_{polymer,surface} = 0$, the conformation data are similar for the two different types of surfaces, but at $RT\chi_{polymer,surface} = \pm 4$ kJ mol$^{-1}$ the results for the two types start to become appreciable (e.g., 50% difference in average length of loops or tails).

**Variation of the Surface Potential/Surface Charge Density.** Finally, we will examine how the adsorption depends on the surface potential ($\psi_0$-surface) or on the surface charge density ($\sigma_0$-surface). As before, Figure 7 shows the adsorbed amount as a function of the salt concentration for a given change in now $\psi_0$ and $\sigma_0$, whereas Figure 11 shows $\Gamma_{ex}$ and $\delta$ as a function of $\psi_0$ and $\sigma_0$ for two different salt concentrations. There is of course a one-to-one correspondence between $\psi_0$ and $\sigma_0$, and Figure 11a shows how the relation can be constructed.

At low $\phi_s$, and as now expected, the adsorbed amount is proportional to the surface charge density (Figures 7b and 11a), whereas for $\phi_s = 10^{-3}$ saturation effects become considerable at $\sigma_0 = -0.1$ ($\tau\Gamma_{ex}/|\sigma_0| = 0.85 < 1$). For constant surface potential, $\Gamma_{ex}$ depends on $\psi_0$ in a more s-like shape. At small potentials $|\psi_0| < 10$ mV, the gain in electrostatic interaction is not sufficient to overcome the loss in configurational entropy upon adsorption. The inflection point occurs at $\approx -50$ mV, and at larger $|\psi_0|$ saturation effects start to emerge, the effect being weaker for $\phi_s = 10^{-5}$ and stronger for $\phi_s = 10^{-3}$. The critical salt concentration for displacing the polyelectrolyte increases with $\psi_0$ and $\sigma$ (cf. also Figure 7).

Figure 11b shows that the thickness reduces with increasing $|\psi_0|$ or $|\sigma_0|$ and levels off at ca. $\psi_0 = -50$ mV or $\sigma_0 = -0.03$, and hence the thickness of the excess amount is largest when the excess amount is at its smallest. This suggests that the loop, tail, and train characteristics do not vary at large values of $|\sigma_0|$ or $|\psi_0|$, and such analyses indeed show that the average length and fraction of segments in loops, tails, and trains remain essentially constant at $|\sigma_0| > 0.05$ or $|\psi_0| > 75$ mV.

## IV. Discussions

**Reference System.** The invariant amount of adsorbed polyelectrolyte at low $\phi_s$ for the $\sigma_0$-surface (Figure 2a) is an effect of the system being in a regime where the adsorbed amount is governed by charge compensation.[12] Table 2 showed that the deviation from perfect charge compensation is indeed very small, $|(\tau\Gamma_{ex} - |\sigma_0|)/\sigma_0| < 10^{-3}$, for the smooth, regular, and random charge distributions at low salt concentration, and the deviation is only marginally larger for the diblock copolymer. Regarding the $\psi_0$-surface, it responses with an increase of the number of charged groups when the adsorption of the polyelectrolyte becomes more favorably for some other reasons. In the present case, for a given chemical potential of the polyelectrolyte in bulk, the free energy of the adsorbed molecules is reduced as the polyelectrolyte charge distribution becomes more uneven, and hence the adsorbed amount is increased. The reason for the free energy reduction is that the adsorption can take place with a smaller loss in chain conformational entropy without reducing the gain in attractive electrostatic interaction energy too much.

The main results of the configuration analysis corroborate with the qualitative description of the adsorbed state at different salt concentrations of polyelectrolytes as given by Fleer et al.[1] At low salt concentration, we have many but short loops which become fewer and longer at increased $\phi_s$. Meanwhile, the tails become more extended, and the number of anchoring points is reduced. However, a noticeable point is that even for $r_{polymer}$ as large as 1000 at low salt concentration, the effects of the tails are considerable for weakly charged polyelectrolytes. The analysis showed that at increasing salt concentration the extended tails cause an increased thickness, despite the fact that the amount of adsorbed polyelectrolyte is reduced. This behavior has experimentally been inferred from the adsorption of a weakly charged cationic polyacrylamide on an oxidized silica surface,[5] but such appearance is not expected to occur for neutral polymers.

In addition, the results show that the smooth representation of the charge distribution previously used[10,12] is an excellent approximation for a polyelectrolyte with a regular charge distribution. But, when modeling polyelectrolytes with a random charge distribution, it becomes more important to explicitly take into account the real charge distribution in the model. Larger discrepancies between regular and random charge distributions than those shown in Figures 2 and 3 were observed in previous model calculations with $r_{polymer} =$ 10 000 and nonelectrostatic surface interactions.[5] In the limiting case of a diblock copolymer with one charged and one uncharged block, the adsorbed polymer forms a brush with extended neutral tails firmly anchored by the charged blocks. Such system has been investigated by Israël both with analytic as well as mean-field lattice approaches.[9]

**Variation of Conditions.** In view of the picture emerged of the adsorbed state of the weakly charged

polyelectrolyte, we will now discuss the results obtained when the length, the linear charge density, and the volume fraction of the polyelectrolyte as well as the nonelectrostatic polyelectrolyte−surface interaction and the surface potential/charge density were varied, all at different salt concentrations.

It was previously concluded that the excess adsorbed amount decreases and the thickness of the adsorbed layer increases upon addition of salt. This qualitative response, a reduction of the amount adsorbed and an increase in the thickness, also holds extremely well when $\chi_{\text{polymer,surface}}$ (Figure 10) or $\psi_0$ or $\sigma_0$ (Figure 11) are varied, *but* for changes in the linear charge density an increase in the excess amount adsorbed is accompanied by an increase in the thickness (Figure 9). Regarding variation in $r_{\text{polymer}}$, the former regime was obtained at low salt concentrations and the latter regime at high salt concentrations (Figure 8), whereas both the adsorbed amount and the thickness were insensitive to changes in $\phi_{\text{polymer}}$.

Thus, a less (effective) attractive polyelectrolyte−surface interaction caused either by (i) increased salt concentration, (ii) less favorable or more unfavorable nonelectrostatic polyelectrolyte−surface interaction, or (iii) smaller magnitude of the surface potential or the surface charge density all leads to a smaller amount adsorbed but to a thicker adsorbed layer. The conformation analyses show that this is accompanied by longer tails, fewer and longer loops, and a smaller number of segments in direct contact with the surface. The opposite variations of $\Gamma_{ex}$ and $\delta$ are possible since the density of the adsorbed layer is small (Figure 5). [However, at sufficiently strong adsorption, the increase in $\Gamma_{ex}$ and the reduction of $\delta$ levels off (most clearly seen in Figure 11).]

The similar response ($\Gamma_{ex}$ and $\delta$ increase simultaneously) obtained for variation of the linear charge density is related to the fact that given the anchoring of the polyelectrolyte is sufficiently strong, a reduction of the fraction of charged segments leads to an increase in the number of adsorbed neutral segments per charged and anchored segment (increased $\Gamma_{ex}$) as well as to longer loops and tails (increased $\delta$). One should note that the rise in the thickness at smaller $\tau$ is not sensitive on the type of surface or salt concentration, whereas the change in excess adsorbed amount is sensitive to both of these parameters. It is also notable that, at such small $\tau$ where the anchoring starts to becomes insufficient for maintaining charge compensation ($\sigma_0$-surface), the increase in the thickness with reduced $\tau$ is *not* affected by the reduction of the adsorbed amount. Thus, again the conformation of the adsorbed polyelectrolytes is not directly affected by the amount adsorbed.

Another important result is the different adsorbed amount obtained for the two types of surfaces as the conditions are changed. The origin of the varying $\Gamma_{ex}$ for the different charge distributions of the model polyelectrolyte was given above, and the same arguments are applied here. Thus, at low salt concentration and at a constant surface charge density, the system tends to keep the surface charges compensated to a very high degree by adsorption of a suitable amount of polyelectrolyte (any deviation is energetically very costly), hence making the excess amount adsorbed independent of (i) the length of the polyelectrolyte, (ii) the volume fraction of the polyelectrolyte, and (iii) the polyelectrolyte−surface interaction, whereas the excess amount adsorbed becomes inversely proportional to the linear charge density and proportional to the surface charged density. Regarding the constant surface potential case at low salt concentration, the amount adsorbed increases as the adsorption becomes more favorable for some reasons, i.e., $\Gamma_{ex}$ increases with increasing $r_{\text{polymer}}$ and $\phi_{\text{polymer}}$ and decreasing $\chi_{\text{polymer,surface}}$. This increase in $\Gamma_{ex}$ is made electrostatically possible by an increase of $|\sigma_0|$ (in order to maintain the constant $\psi_0$), and in all cases with low salt concentration, there is an almost complete matching of the adjusted surface charge and the polyelectrolyte charge. Many qualitative differences between the constant surface potential and constant surface charge density are reduced as the salt volume fraction becomes high. However, quantitative sizable differences still exist (cf. Figures 8 and 9).

Finally, this investigation has been restricted to changes in at most two system parameters ($\phi_s$ + another) simultaneously for two types of surfaces. A study of the adsorbed state using another reference system or simultaneous variation of a larger number of system parameters would complement the picture obtained here. For example, in our previously work, where $r_{\text{polymer}} = 10\,000$ and $\psi_0 = -100$ mV with nonelectrostatic surface interactions were used, $\Gamma_{ex}$ vs $\phi_s$ displayed a distinct maximum and $\delta$ could increase 5-fold upon salt addition.[5] Moreover, the study by van de Steeg et al. also dealt with the effects of specific adsorption of polymer segments and salt species.[12]

## V. Conclusions

On the basis of mean-field lattice calculations, the adsorption of weakly charged and flexible polyelectrolytes at oppositely charged and planar surfaces has been investigated. In general, weakly charged polyelectrolytes display a much richer variation of the adsorbed state as compared to highly charged polyelectrolytes.

Two limiting cases, constant surface potential and constant surface charge density, have been considered throughout. In the latter case, the amount adsorbed is controlled by charge compensation at not too high salt concentration, whereas for constant surface potential the picture is more complex.

Upon addition of salt, the excess adsorbed amount is reduced and the thickness of the adsorbed layer is increased, resulting in a less dense but spatialy more extended adsorption layer. Similar response is obtained when an unfavorable polyelectrolyte−surface interaction is introduced or when the magnitude of the charge or potential of the surface is reduced. An increase of the linear charge density of the polyelectrolyte generally reduces the amount adsorbed as well as the thickness of the adsorbed layer, whereas the the influence of the length of the polyelectrolyte on the adsorption is less regular and the effect of the polyelectrolyte volume fraction is very small.

It was found that the polyelectrolyte charge distribution has a substantial influence on the adsorption. A random charge distribution gives a higher adsorbed amount, larger thickness, and stronger segment segregation as compared to a regular distribution.

At low salt concentrations, in the absence of nonelectrostatic polyelectrolyte−surface interaction, and in the case of the random charge distribution, the charge of the surface was overcompensated by the polyelectrolyte charges, but the degree of overcompensation is minute. However, at not too high salt concentration the electro-

static potential typically changes sign some 10 layers from the surface, signaling a reversal of the total charge.

It should be kept in mind that the results discussed here originate from a model with its defined approximations. For example, the mean-field approximation affects the amount adsorbed both through the effects close to the surface and those in the bulk. In the former case spatial correlations are admissible between the layers but neglected within them. In bulk all spatial correlations are neglected which affects the chemical potential and hence the amount adsorbed at a given bulk volume fraction. In our treatment we have also assumed flexible polyelectrolytes. As the intrinsic stiffness (stiffness at high salt concentration) increases, it is anticipated that the adsorbed amount increases. A less flexible polymer has less configurational entropy to lose when being close to a surface. Despite these shortcomings, the present results should hold qualitatively and be useful for providing a guidance of how to modify systems in order to achieve desired changes in different properties.

**Acknowledgment.** This work was supported by the Swedish Research Council for Engineering Science (TFR).

## References and Notes

(1) Fleer, G. J.; Cohen Stuart, M. A.; Scheutjens, J. M. H. M.; Cosgrove, T.; Vincent, B. *Polymers at Interfaces*; Chapman & Hall: London, 1993; p 502.
(2) Lindström, T.; Wågberg, L. *Tappi J.* **1983**, *66*, 83.
(3) Wang, T. K.; Audebert, R. *J. Colloid Interface Sci.* **1988**, *121*, 32.
(4) van de Steeg, H. G. M.; de Keizer, A.; Cohen Stuart, M. A.; Bijsterbosch, B. H. *Colloids Surf. A: Physicochem. Eng. Aspects* **1993**, *70*, 77.
(5) Shubin, V.; Linse, P. *J. Phys. Chem.* **1995**, *99*, 1285.
(6) Hesselink, F. Th. *J. Colloid Interface Sci.* **1977**, *60*, 448.
(7) Muthukumar, M. *J. Chem. Phys.* **1987**, *86*, 7230.
(8) Åkesson, T.; Woodward, C.; Jönsson, B. *J. Chem. Phys.* **1989**, *91*, 2461.
(9) Israëls, R. Thesis, Wageningen, 1994.
(10) Böhmer, M. R.; Evers, O. A.; Scheutjens, J. M. H. M. *Macromolecules* **1990**, *23*, 2288.
(11) Borisov, O. V.; Zhulina, E. B.; Birshtein, T. M. *J. Phys II (Fr.)* **1994**, *4*, 913.
(12) van de Steeg, H. G. M.; Cohen Stuart, M. A.; de Keizer, A.; Bijsterbosch, B. *Langmuir* **1992**, *8*, 2538.
(13) Beltrán, S.; Hooper, H. H.; Blanch, H. W.; Prausnitz, J. M. *Macromolecules* **1991**, *24*, 3178.
(14) Granfeldt, M. K.; Jönsson, B.; Woodward, C. E. *J. Phys. Chem.* **1991**, *95*, 4819.
(15) Dahlgren, M. A. G.; Waltermo, Å.; Blomberg, E.; Claesson, P. M.; Sjöström, L.; Åkesson, T.; Jönsson, B. *J. Chem. Phys.* **1993**, *97*, 11769.
(16) Wallin, T.; Linse P. *Langmuir*, in press.
(17) Scheutjens, J. M. H. M.; Fleer, G. J. *J. Phys. Chem.* **1979**, *83*, 1619.
(18) Scheutjens, J. M. H. M.; Fleer, G. J. *J. Phys. Chem.* **1980**, *84*, 178.
(19) Flory, P. J. *Principles of Polymer Chemistry*; Cornell University Press: Ithaca, NY, 1953.
(20) Linse, P.; Björling, M. *Macromolecules* **1991**, *24*, 6700.
(21) Dahlgren, M. A. G.; Claesson, P. M.; Audebert, R. *J. Colloid Interface Sci.* **1994**, *166*, 343.

MA950539V